Carbohydrate Polymers 114 (2014) 141–148

Contents lists available at ScienceDirect

Carbohydrate Polymers

journal homepage: www.elsevier.com/locate/carbpol

Maltose-conjugated chitosans induce macroscopic gelation of pectin solutions at neutral pH

D. Giacomazza[a,*], M.A. Sabatino[b], A. Catena[c,1], M. Leone[a,c], P.L. San Biagio[a], C. Dispenza[a,b]

[a] Istituto di Biofisica (Palermo Unit), Consiglio Nazionale delle Ricerche, via U. La Malfa, 153, 90146 Palermo, Italy
[b] Dipartimento di Ingegneria Chimica, Gestionale, Informatica, Meccanica, Università di Palermo, Viale delle Scienze, Building 8, 90128 Palermo, Italy
[c] Dipartimento di Fisica e Chimica, Università di Palermo, Viale delle Scienze, Building 17, 90100 Palermo, Italy

ARTICLE INFO

Article history:
Received 26 February 2014
Received in revised form 30 July 2014
Accepted 1 August 2014
Available online 17 August 2014

Keywords:
Maltose-conjugated chitosan
Hydrogels
Pectin
Biocompatible materials
Rheology

ABSTRACT

Injectable polymer scaffolds are particularly attractive for guided tissue growth and drug/cell delivery with minimally invasive intervention. In the present work, "all-polymeric" gelling systems based on pectins and water-soluble maltose-conjugated chitosans (CM) have been developed. Maltose-conjugated chitosan has been synthesized at three different molar ratios, as evaluated by FITR analysis and fluorimetric titration. A thorough rheological characterization of the blends and their parent solutions has been performed. Macroscopic gelation has been achieved by mixing the high esterification degree pectins with CM at higher maltose grafted to chitosan contents. Gels form in a few minutes and reach their full strength in less than two hours. These features encourage their further development as scaffold for tissue engineering.

1. Introduction

Recent advances in regenerative medicine are setting up a great demand of more and better performing biocompatible, self-aggregating materials and structures, with the purpose of creating the required support for repairing damaged/defective human tissues with minimal or no recourse to surgical intervention (Karp & Langer, 2007). For the purpose of scaffolding, biomaterials that are able to undergo sol–gel transitions in physiological conditions are highly desirable. Polymeric gels are elective materials for scaffolding in consideration of the high flexibility of their chemical structures, the availability of functional groups for bio-derivatization reactions and their similarities with many natural tissues as for water content and mechanical properties.

Depending on their chemical composition, polymeric gels can undergo sol–gel transitions as a response of a variation of temperature from ambient to body temperature (Lee et al., 2010), in the presence of specific ions (Wang, Zhang, Konno, & Saito, 2004), by interaction with UV light (Pitarresi, Giacomazza, Triolo, Giammona, & San Biagio, 2012) and other radiation sources (Dispenza, Battaglia, Licciardi, Giammona, & Spadaro, 2005; Dispenza, Alessi, & Spadaro, 2009; Dispenza et al., 2010, 2012; Sabatino et al., 2013) or by mixing with a second polymeric compound (Hori, Winans, & Irvine, 2009). Sol–gel transitions of polymeric systems can be exploited to engineer in-situ gelling formulations. These formulations can be administered in a straightforward manner, through injection. They are able to fill cavities and be shaped in complex forms, and access almost any compartment in the human body.

Indeed, there are a number of challenges that still need to be meet. Often the starting point is a physiological solution of the polymer. Homogeneous aqueous polymer systems are not always easy to prepare and not always stable upon storage. Low viscosity solutions at room temperature are highly desirable to minimize the risk of the syringe clogging upon injection and to completely fill the cavity in which they have been injected, despite its irregular shape. Once in situ, the solutions should undergo a relatively rapid sol–gel transition, to remain confined in the injection locus without diffusing out in the surrounding tissues. The progressive resorption of the scaffold must occur in a temporal time scale that matches the one for new tissue formation and vascularization (Sokolsky-Papkov, Agashi, Olaye, Shakeshef & Domb, 2007).

* Corresponding author. Tel.: +39 091 6809335; fax: +39 091 6809312.
E-mail addresses: daniela.giacomazza@cnr.it (D. Giacomazza), mariaantonietta.sabatino@unipa.it (M.A. Sabatino), albertoc.89@hotmail.it (A. Catena), clelia.dispenza@unipa.it (M. Leone), pierluigi.sanbiagio@cnr.it (P.L. San Biagio), clelia.dispenza@unipa.it (C. Dispenza).
[1] Present address: University Koblenz-Landau, Campus Koblenz, Institute for Integrated Natural Sciences, Department of Physics, Universitätsstraße 1, D-56070 Koblenz, Germany.

http://dx.doi.org/10.1016/j.carbpol.2014.08.014
0144-8617/

Natural biopolymers have been often proposed as main constituents of hydrogel scaffolds due to their biocompatibility, prevalence and non-immunogenic effect (Chajra et al., 2008; Collins & Birkinshaw, 2013; Croisier & Jerome, 2013; Glowacki & Mizuno, 2008; Ravi Kumar, Muzzarelli, Muzzarelli, Sashiwa, & Domb, 2004; Leach, Bivens, Patrick, & Schmidt, 2003; Lei, Rahim, Ng, & Segura, 2011; Munarin et al., 2011; Rinaudo, 2006; Seidlits et al., 2011). The great variety of polymeric structures available, as for composition, topological features and supramolecular organization, has a counterpart in both feedstock and batch-to-batch variability and in the great influence that the purification procedure has on the chemical and physical properties of the materials (Lanza, Langer, & Vacanti, 2000). Most of the hydrogel scaffolds are based on hyaluronic acid (Leach et al., 2003; Lei et al., 2011; Seidlits et al., 2011; Collins & Birkinshaw, 2013), collagen (Glowacki & Mizuno, 2008; Chajra et al., 2008), chitosan (Croisier & Jerome, 2013; Ravi Kumar et al., 2004; Rinaudo, 2006), alginate (Wang, Yang, Lin, Liu, & Lin, 2011) and pectin (Munarin et al., 2011).

In the present article, we show the rheological behavior of formulations obtained by mixing two polymer aqueous solutions. One contains pectin, either a low methoxy (LM) or a high methoxy (HM) variant, and the other comprises a maltose-linked-chitosan. In particular, the chemical modification of chitosan with maltose was performed to extend its solubility range in water from low to neutral pH.

Chitosan, the cationic (1–4)-2-amino-2-deoxy-β-D-glucan, has typical degree of acetylation close to 0.20. It is produced from chitin-bearing fishery by-products (Muzzarelli, 1977, 2012; Muzzarelli et al., 2012). Certain chitosan salts are water-soluble. The chemical modification of chitosan in general takes advantage of the reactivity of the primary amino groups, thus various mono- and di-saccharide units have been linked to it (Kurita, Akao, Kobayash, Mori, & Nishiyama, 1997; Kurita, Akao, Yang, & Shimojoh, 2003; Yalpani & Hall, 1984). Those reactions extend the solubility range of chitosan and, in particular, the chitosan–maltose derivative remains soluble in water at pH values close to 10 (Kurita et al., 2003).

Pectin is a heterogeneous polysaccharide whose main constituent is a linear sequence of 1,4-linked α-D-galactopyranosyluronic units with some of the carboxyl groups esterified with methanol. Depending on the proportion of methyl ester groups present in the polymeric chain, pectin is classified as high methoxy (HM) having 50% or higher esterification degree (DE), or low methoxy (LM), having 50% or lower esterification degree. HM pectin may form a gel at acid pH (lower than 3.5) only in the presence of large amounts of sugars or other co-solutes and its complex gelation mechanism involves the formation of junction zones stabilized by hydrophobic interactions and H-bonds (Oakenful, 1991; Bulone, Giacomazza, Manno, Martorana, & San Biagio, 2010). In the case of LM pectin, the gel formation is ionic-mediated through divalent cations, the most relevant being the Ca^{++}. The proposed mechanism for LM pectin gelation is the so-called "egg-box model" (Grant, Morris, Rees, Smith, & Thom, 1973) in which the positive ion lies in the cavity formed by two adjacent pectin ribbons. Interruptions with 1,2 linked L-rhamnose residues make the backbone irregular and provide kinks responsible for its flexibility. Pectin with DE close to 50 shows a behavior in between HMP and LMP.

The characteristics of chitosan and pectin, including non-toxicity (Muzzarelli & Muzzarelli, 2009; Yamada, 1996) antibacterial activity (Birch & Schiffman, 2014) and biodegradability (Mishra, Banthia, & Majeed, 2012; Croisier & Jerome, 2013), make these polysaccharides attractive for scaffolding applications. Neither of these polymers can undergo gelation at physiological pH and body temperature, and without the addition of significant amounts of low molecular weight co-solutes, such as salts, sugar, and alcohols. An "all-polymeric" gelling system should offer a better toxicological profile and minimal interference with cell functions.

In this work we explored the possibility of forming pectin gels, at physiological temperature and neutral pH, by mixing equal volumes of pectin aqueous solutions and low-concentrated maltose-conjugated chitosan aqueous dispersions. In particular, maltose-chitosan adducts at different derivatization degrees were synthesized to promote water dispersibility of chitosan at neutral pH. The synthetic approach has adapted from Holme and Hall (1992) and the products have been characterized for their chemical functionality and rheological behavior to support the occurrence of chemical modification and understand their supra-molecular organization in water, respectively. The influence of esterification degree and concentration of pectin on gel strength has been also investigated.

2. Experimental

2.1. Materials

All reagents were of the best available commercial grades. Glacial acetic acid (≥99.7%), low molecular weight chitosans (DA > 80% and DA > 90%), sodium cyanoborohydride (95%), methanol CROMASOLV (HPLC grade) were from Sigma Aldrich. 31%, 59% e 65% DE pectins are a kind gift from Hercules Inc. Milli *Q* water was used for both systems preparation and purification.

2.2. Synthesis of chitosan–maltose derivatives and sample preparation

Chitosan–maltose (CM) derivatives were synthesized as described by Yalpani and Hall (1984) and Holme and Hall (1992). In particular, in the case of CM 1:1, chitosan was dissolved in a 100 ml mixture (1:1 by volume) of methanol and 0.2 M acetic acid under magnetic stirring, to obtain a final chitosan concentration of 0.2 wt% 10 ml of the maltose (0.4 M) and sodium cyanoborohydride (5×10^{-3} M) solution was added with vigorous stirring. The reaction mixture was left stirring at room temperature for 2 days. The products were extensively (10 days) dialyzed against Milli *Q* water to eliminate added solutes and excess maltose. Samples with different maltose/chitosan molar ratio were obtained by modifying the stoichiometric amount of reactants. After dialysis, aliquots of the different systems were weighed and lyophilized to obtain the concentrations of the final samples. Final concentrations were comprised between 0.15 wt% and 0.17 wt%.

All samples were used at the final concentration of 0.15 wt%, by diluting with Milli *Q* water if necessary. The pH of the final solutions was 6.8. All samples were always stored at 4 °C before use.

2.3. Pectin sample preparation

31%, 59% and 65% DE pectin solutions at the concentrations of 1 wt%, 2 wt% or 4 wt% were prepared by dissolving the powder in Milli *Q* water at 100 °C for 10 min under magnetic stirring. The solutions were then cooled at room temperature overnight, stored at 4 °C and used up to 3 days.

2.4. Preparation of samples of chitosan–maltose derivatives and pectins

Maltose-conjugated chitosans and pectin systems were obtained by mixing equal volumes of each of the three chitosan–maltose systems (0.15 wt%) and pectin, at different concentrations (1, 2 or 4 wt%) and different esterification degrees (31%, 59% and 65%) at room temperature for 1 min and

placed directly on the rheometer's plate set at the physiological temperature of 37 °C.

2.5. FTIR analysis

FTIR measurements on all samples were carried out on the Perkin-Elmer-Spectrum 400 apparatus by dispersing the dry materials in potassium bromide and compressing them into pellets. In particular, the CMs systems were characterized after dialysis and freeze–drying, while the unmodified chitosan was first dissolved in aqueous acetic acid (0.2 M), dialyzed and then freeze-dried. Spectra were recorded at 32 scans per spectrum and 1 cm^{-1} resolution in the 4000–400 cm^{-1} range.

2.6. Fluorimetric titration of chitosan primary amino groups

The derivatization degree of the maltose-conjugated chitosan has been determined from the difference between the concentration of primary amino groups present in chitosan and their residual amount after conjugation with maltose. For this purpose a chitosan with DA > 90% has been used. Reaction of primary amino groups with fluorescamine produces a fluorescent adduct with a maximum emission at 480 nm (excitation wavelength of 392 nm) (Chen & Zhang, 2011; Toome & Manhart, 1975). Fluorescence spectra were recorded on an FP-8200 Spectrofluorometer (Jasco). A calibration curve was built using chitosan (DA > 90%) solutions reacted with fluorescamine at different concentrations.

2.7. Rheological measurements

The rheological measurements were carried out on a TA Instruments AR-G2 rheometer at the temperatures, controlled by Peltier system, of 20 °C or 37 °C, ±0.1. The geometry was a plate–acrylic cone system with a diameter of 40 mm and a gap of 30 μm. Frequency sweep cycles have been recorded for a period of 24 h; a pause of 30 min between consecutive measurements in order to avoid mechanical perturbation of the sample was fixed. Mechanical spectra were performed in the range 0.02–30 Hz with a strain of 0.02.

Flow curves were performed in the range 0.1–5000 s^{-1} shear rate with the same geometry. Time sweep measurements were done using a plate–acrylic plate geometry (diameter 40 mm, gap 1000 μm) at the frequency of 1 Hz, strain 0.02. The thin sample-air interface has been coated with silicon oil to avoid evaporation. All measurements have been performed at least in triplicate.

2.8. SEM analysis

The morphology of dried macrogel has been investigated by a field emission scanning electron microscopy (FESEM) system (JEOL) at an accelerating voltage of 10 kV. The samples have been frozen in liquid nitrogen for 15 min, lyophilized to obtain a perfectly dried material, placed on the stub and gold-sputtered.

3. Results and discussion

3.1. Structural properties and rheological behavior of maltose-conjugated chitosans

Maltose-conjugated chitosan dispersions were characterized for their chemical structure by FTIR analysis (Fig. 1A and B. In Fig. 1A the spectra of a typical conjugated chitosan, maltose and unmodified chitosan are reported, while in Fig. 1B the comparison among the spectra of CM 1:3, CM 1:1 and CM 3:1 variants is shown. The spectral modifications of chitosan, as a result of the conjugation with maltose, consist in: (i) the increase of the bands associated to the stretching and bending vibrations of bound hydroxyl groups at 3398 cm^{-1} and 1263 cm^{-1}, respectively; (ii) the reduction of the absorption bands at 1601 cm^{-1}, attributed to primary amine group stretching vibration and (iii) the increase of the absorptions at 1155 cm^{-1} and 1079 cm^{-1}, related to the ν_{as} and ν_s of C—O—C and C—O, respectively. These modifications support the occurrence of chemical grafting of maltose to chitosan via depletion of amino groups and increase of hydroxyl and ether functionalities. From Fig. 1B, it is evident that the increase of maltose content with respect to chitosan in the reactor feed leads to a progressively higher grafting degree of the sugar to the polysaccharide chain. The conjugation degree was also estimated by fluorimetric titration resulting about 22%, 45% and 55% for CM 3:1, CM 1:1 and CM 1:3, respectively.

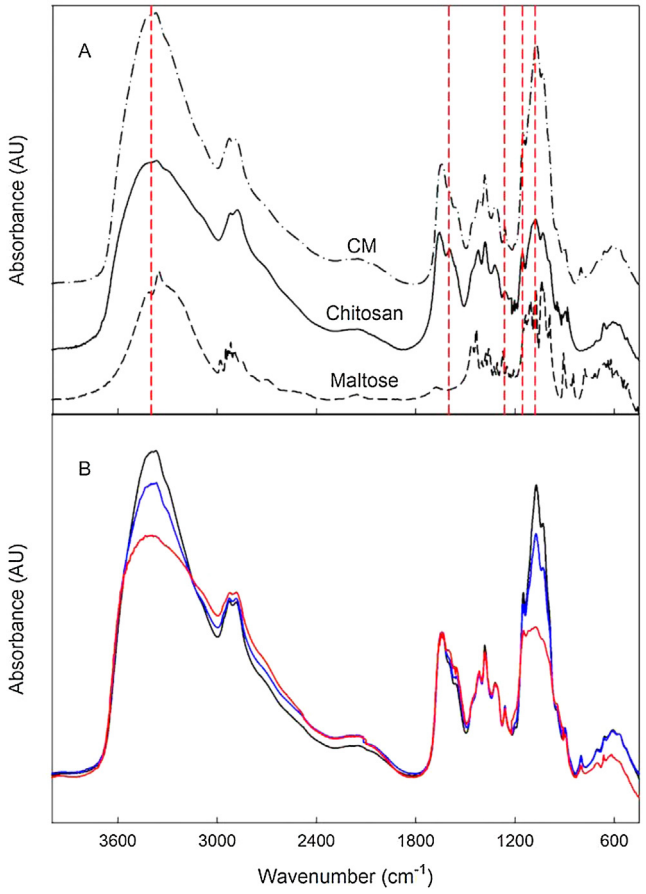

Fig. 1. *FT-IR analysis*—(A) Comparison among FT-IR spectra of maltose (dashed line), chitosan (solid line) and maltose-conjugated chitosan (CM, dashed–dotted line). (B) Spectra of CM 3:1 (red line), CM 1:1 (blue line) and CM 1:3 (black line). (For interpretation of the references to color in this figure legend, the reader is referred to the web version of this article.)

The rheological behavior of aqueous maltose-conjugated chitosans was investigated as a function of time at two temperatures, 20 and 37 °C. Mechanical spectra cycles were collected over 24 h. Fig. 2A–F report the first (left column) and the last (right column) frequency run recorded at 20 °C and 37 °C, respectively. Although all systems appear liquid and easy-to-inject, from a rheological point of view, they exhibit a very weak gel-like character. Indeed, G' values are always higher than G'' and frequency-independent, indicating that the polymers have a self-organized structure, in agreement with the definition of Almdal, Dyre, Hvidt, and Kramer (1993). Furthermore, the comparison of the mechanical spectra, which refer to the two temperatures, suggests that the degree of supramolecular organization is higher the higher is temperature

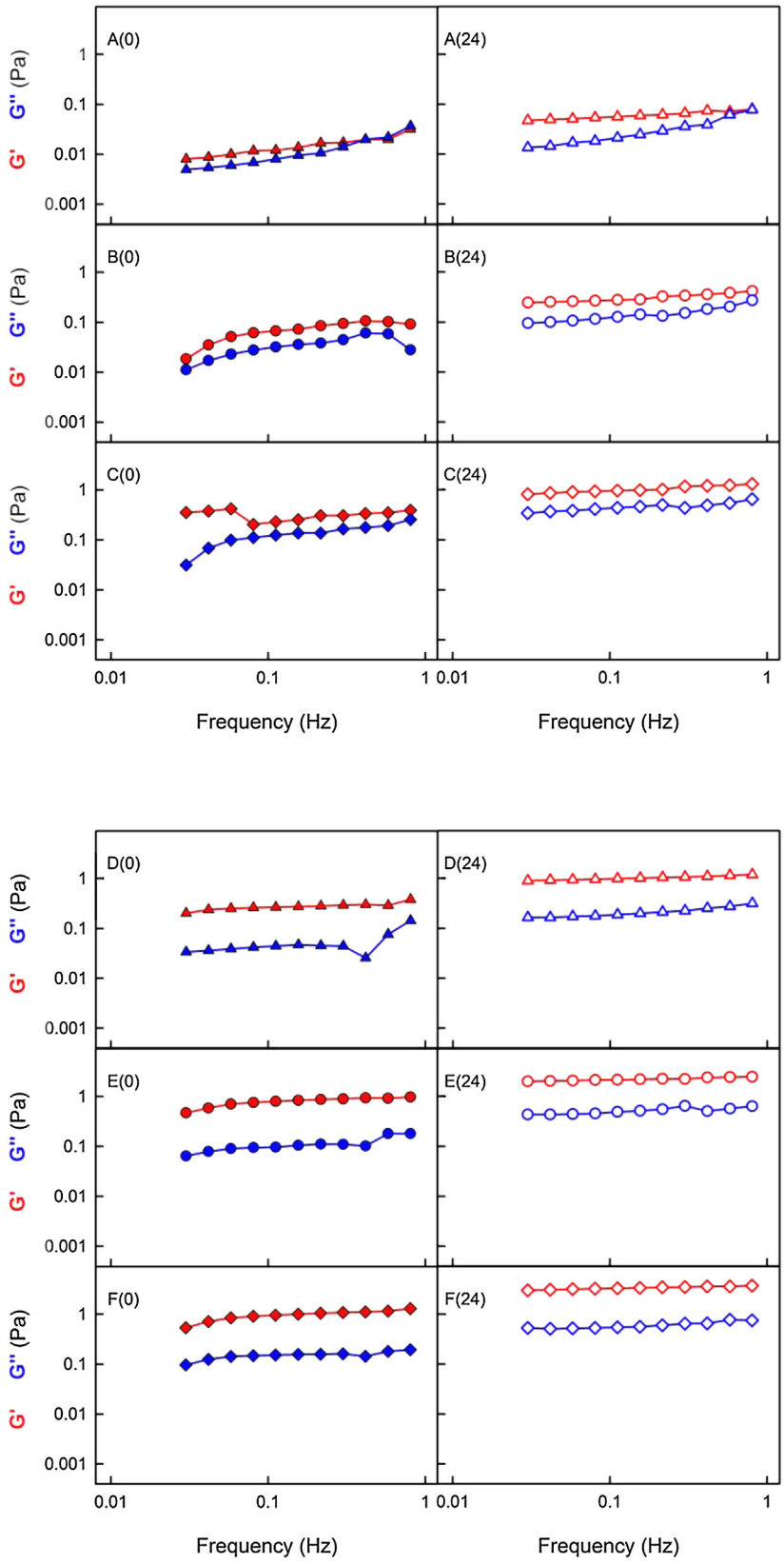

Fig. 2. *Maltose-conjugated chitosan mechanical spectra—G′* (red simbols) and *G″* (blue symbols) values recorded during the first (A(0), B(0), C(0), D(0), E(0) and F(0)) and the last (A(24), B(24), C(24), D(24), E(24) and F(24)) run of the cycles of mechanical spectra obtained for CM 1:3 ((A) and (D)), CM 1:1 ((B) and (E)) and CM 3:1 ((C) and (F)), 0.15 wt%, at the temperature of 20 °C ((A)–(C)) and 37 °C ((D)–(F)) monitored for 24 h. (For interpretation of the references to color in this figure legend, the reader is referred to the web version of this article.)

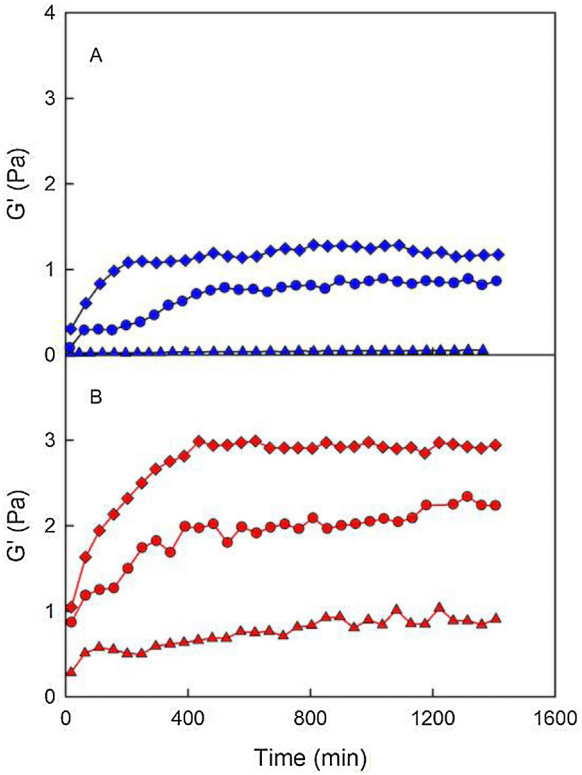

Fig. 3. *Kinetic measurements*—Kinetic profiles at 20 °C (A) and 37 °C (B) obtained for CM 1:3 (triangles), CM 1:1 (circles) and CM 3:1 (diamonds), 0.15 wt%, at the frequency of 0.2 Hz, recorded for 24 h.

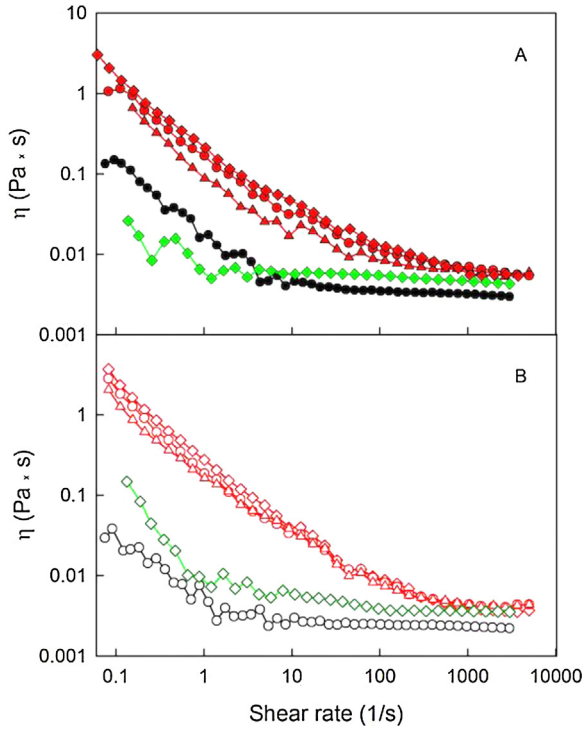

Fig. 4. *Viscosity comparison*—Flow curves obtained for CM 3:1 (red diamonds), CM 1:1 (red circles), CM 1:3 (red triangles) 0.15 wt% in water and CM 1:3 (green diamond) and chitosan (black circles) 0.15 wt% in acetic acid 0.2 M at 20 °C (A) and 37 °C (B). (For interpretation of the references to color in this figure legend, the reader is referred to the web version of this article.)

(Ross-Murphy, 1995). This result is better evidenced in Fig. 3A and B, where G' values at a given frequency are reported as a function of time, for the two explored temperatures. G'' values are not reported for clarity, but are always lower than G'. These plots were made with data extracted from the mechanical spectra repeatedly acquired over 24 h, as described above. All systems show a progressive increase of storage modulus with time, with the exception of CM 1:3 at 20 °C. As a general trend, the aggregation propensity is more pronounced for the variants with lower sugar content. Expectedly, maltose short branches increase the affinity of chitosan toward water, due to the increased hydrophylicity and induced flexibility, hence lower packing ability, of the polysaccharide chains which can, in turn, favor multiple hydrogen bonding interactions with the solvent (Baek, Yoo, & Lim, 2003). It can be observed that all samples reach a plateau value within 24 h and, for the least conjugated system (CM 3:1), the plateau is attained in 3.5 h and 4.5 h at 20 and 37 °C, respectively. It is also interesting to observe that the temperature does not increase the aggregation rate, as much as it affects the G' values. For any of the systems investigated, the extent of the aggregation is higher the higher is the temperature, thus suggesting a diffusion-controlled phenomenon.

In order to better elucidate the nature of interactions among CM chains in water, mechanical spectra were also performed on the system with the highest polymer/maltose molar ratio, CM 3:1, dissolved in acetic acid. Frequency runs for the two investigated temperatures of 20 °C and 37 °C (data not shown) indicate that, under these experimental conditions, the polymer exhibits a typical liquid-like behavior with $G' < G''$ and a noticeable frequency dependence (Kavanagh & Ross-Murphy, 1998). No evolution of the spectra was also observed during 24 h of repeated testing. Ionization of the residual NH_2 groups, achieved in the presence of acetic acid in water, reduces the hydrophobicity of the polymer and introduces electrostatic repulsions among CM chains, thus inhibiting the aggregation process. This evidence also confirms the dominant physical nature of the interactions that drive aggregation and rule out any significant contribution from chemical intermolecular crosslinking, which could have occurred upon the conjugation reaction with maltose, if two chitosan chains reacted with the same maltose molecule (leading to inter-molecular bridging instead of grafting).

On the basis of the above results, all further investigations were performed on water polymer aqueous solutions previously incubated for 24 h at 20 °C or 37 °C, in order to allow the attainment of invariant rheological conditions, or otherwise stored at 4 °C.

Maltose-conjugated chitosan systems were also investigated by viscosity measurements and flow curves are reported in Fig. 4A and B for the two temperatures of 20 °C and 37 °C, respectively. The behavior of all CMs is characterized by a strong dependence of viscosity on shear rate. The second Newtonian plateau, η_∞, is only a very small portion of the curve at higher shear rate and it is not affected by the derivatization degree of chitosan amino groups with maltose. The progressive reduction of viscosity at the increase of shear rate is possibly caused by the disentanglement of CM aggregates in water (Lefebvre & Doublier, 2005).

Measurements performed on CM 1:3 and chitosan systems prepared in 0.2 M acetic acid show a reduction of the viscosity value and an extension of the Newtonian plateau, which confirms the partial dissolution of the aggregates. Furthermore, from the comparison of these two curves it appears that the derivatization reaction causes only a slight increase of the Newtonian plateau and hence of the hydrodynamic radius of the polymer.

3.2. Rheological behavior of pectin solutions

Fig. 5 reports the flow curves obtained for pectin solutions at three different esterification degrees and three different

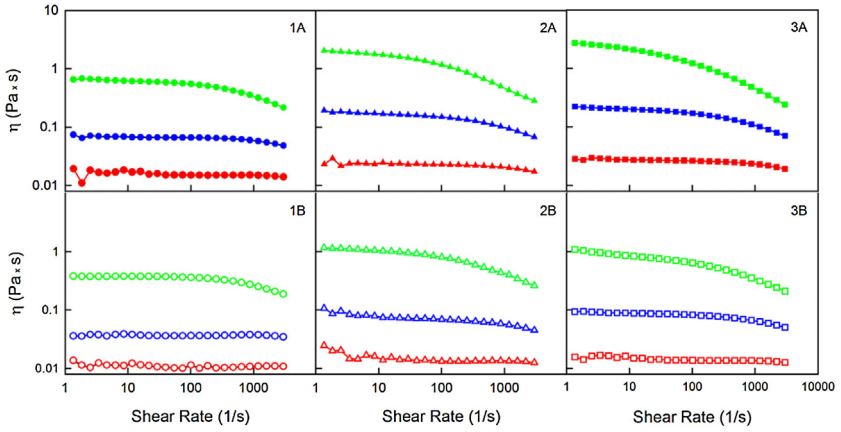

Fig. 5. *Pectin viscosity*—Flow curves obtained for Pectin 31% DE (1), 59% DE (2) and 65% DE (3) at the concentrations of 1 wt% (red symbols), 2 wt% (blue symbols) and 4 wt% (green symbols) at 20 °C (full symbols) and 37 °C (empty symbols). (For interpretation of the references to color in this figure legend, the reader is referred to the web version of this article.)

concentrations. It can be noted a departure from the Newtonian behavior at increasing the concentration and the esterification degree of the polymer. Pectin solutions at 1 wt% show a constant viscosity in almost the whole shear rate range values, independently on the esterification degree. Furthermore, viscosity values obtained on 31% DE pectin are lower than those recorded for higher DE pectins. The behavior can be explained considering that LM pectin adopts in solution a more rigid conformation than HMP (Morris, Foster, & Harding, 2000) and this causes the lowering of the viscosity. Mechanical spectra performed on the same samples and recorded for 24 h exhibited a classic liquid-like viscoelastic behavior and did not show any change at the two different explored temperatures as a function of time (data not shown).

3.3. Structural and rheological behavior of pectin and maltose-conjugated chitosan blends

All the maltose-conjugated chitosans were blended with the three different HM pectin solutions, at the three different concentrations. Since HM-pectin undergoes macroscopic gelation in presence of high amount of cosolutes, such as alcohols or sugars, preliminary measurements were performed to investigate whether maltose at the concentration corresponding to approximately twice as much as the maximum grafted amount to chitosan, obtained for CM 1:3, was able to cause pectin gelation. In these experimental conditions no macroscopic gelation was observed.

Out of the twenty seven mixtures only those prepared with the higher DE pectins (59%, 65%) at 2 and 4 wt% and the higher maltose-conjugated chitosans (1:1 and 1:3) form macrogels. The existence of a concentration threshold is often required for sol–gel transition. For these systems a total polymer content above ca. 1 wt% is required to observe macroscopic gelation. The evidence that gelation occurs only for blends of the higher methoxylated pectins and the higher maltose-conjugated chitosans suggests that a proper balance between hydrophilic and hydrophobic features in each of the two components is required. The macroscopic appearance of gelled samples is homogeneous and opaque.

FTIR analysis performed on the blends that undergo gelation show that the fingerprint of these systems is given by pectin, by far the main component in the systems (97 and 94 wt%) (Coimbra, Barros, Barros, Rutledge, & Delgadillo, 1998).

Fig. 6A and B shows the evolution of the rheological parameters, G' and G'', as a function of time at 37 °C and the mechanical spectrum obtained at the end of the kinetic measurements (100 min) for the sample obtained after mixing the solution of 59% DE pectin at 4% with maltose–chitosan at molar ratio of 1:1, respectively. It can be observed that G'–G'' crossover is located after about 5 min from the beginning of the measurement and both curves attain a plateau after ca. 100 min. The final gel-like structure is characterized by a storage modulus, G', higher than the loss modulus, G'', and almost invariant with the frequency within three decades of frequency (Almdal et al., 1993; Grillet, Wyatt, & Gloe, 2012). This behavior was qualitatively similar for all systems.

G' values for all formulations that exhibited macroscopic gelation are reported in Table 1. The gel strength is relatively higher for systems prepared at the highest total polymer content. Furthermore, the highest G' is achieved for the system formed by

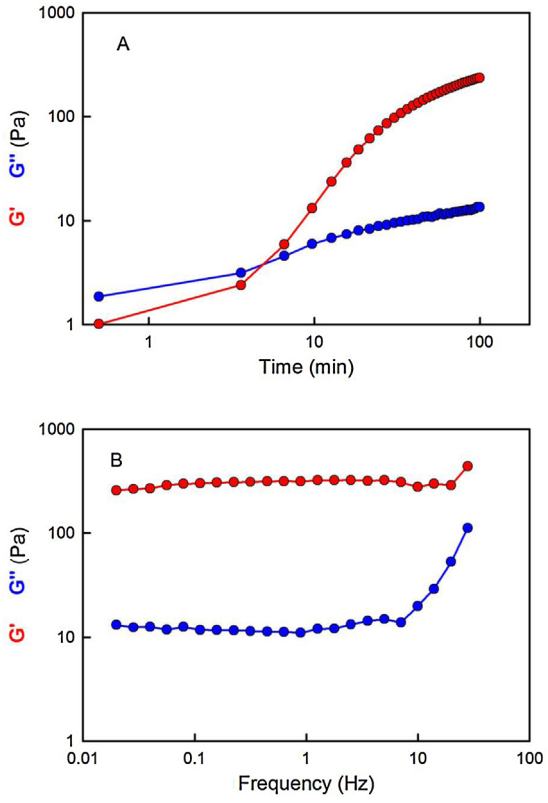

Fig. 6. *Gel formation*—(A) Time evolution of G' (red symbols) and G'' (blue symbols) for CM 1:1, 0.5 wt%, and pectin, 4 wt% 59% DE, at 37 °C recorded at the frequency of 1 Hz. (B) Mechanical spectra obtained at the end of the kinetic measurement (100 min) for the same system at 37 °C (symbols as in (A)). (For interpretation of the references to color in this figure legend, the reader is referred to the web version of this article.)

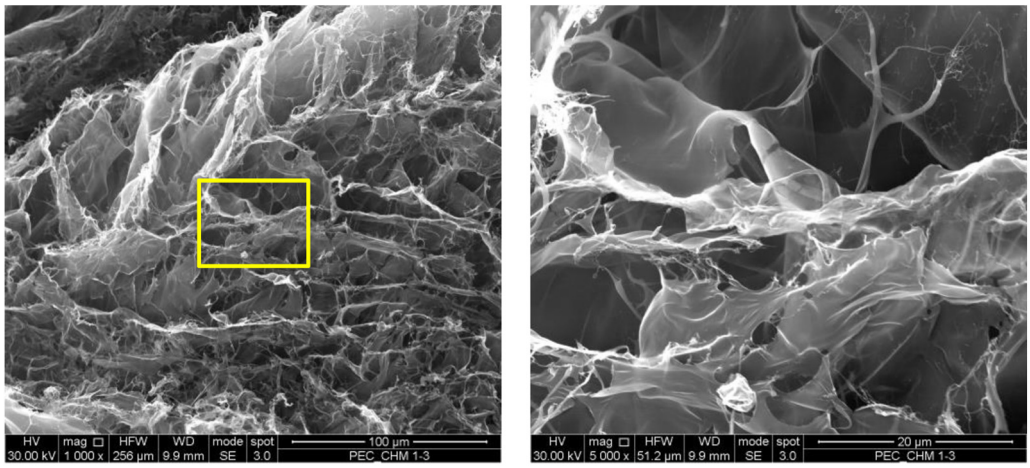

Fig. 7. *SEM experiments*—(A) SEM image of the gel obtained by mixing CM 1:1, 0.15 wt%, and pectin, wt% 59% DE at 37 °C. (B) Magnification of the region in the square.

Table 1
G'' values from kinetic measurements for samples exhibiting macroscopic gelation, as obtained after 100 min from the beginning of the measurement at the temperature of 37 °C and the frequency of 1 Hz.

		Pectin 2 wt%		Pectin 4 wt%	
		59% DE	65% DE	59% DE	65% DE
G' values at 37 °C (Pa)	CM 1:1	**51.00**	**11.33**	**238.40**	**56.24**
	CM 1:3	**46.90**	**15.58**	**165.70**	**39.44**

the pectin with an intermediate DE and the maltose-conjugated-chitosan with an intermediate degree of derivatization. Therefore, gel strength also strongly depends on the right balance between hydrohilicity/hydrophobicity of the two polymers and their residual amino and carboxyl groups. The mechanism of gelation is not fully understood yet and it will be the subject of further investigation.

SEM images obtained on the freeze-dried residue of a typical gel are reported in Fig. 7. All systems show irregular porosity, with larger cavities of tens of microns and smaller pores of only few microns. Increasing the concentration of polymer, the prevailing effect is reducing the dimensions of the larger cavities.

4. Conclusions

Despite their low viscosity values, maltose-conjugated chitosans, as obtained at the three different synthesized molar ratios, form micro-aggregates with a gel-like character, that is more pronounced at 37 °C than at 20 °C. The aggregation propensity is inversely related to the sugar content. The addition of pectin solutions of medium to high esterification degree, causes the formation of the macroscopic network in a few minutes, whereas the systems develop their full strength in less than 2 h. The highest storage modulus attained is of ca. 250 Pa. Further experiments are in progress in order to better clarify the mechanism of gelation of these systems and to evaluate them as scaffolds for soft-tissues regeneration.

Acknowledgements

The authors wish to thank PON MIUR grant no. 01_01287 “SIB: Soluzioni avanzate basate su biomateriali a matrici composite complesse per la riparazione e la rigenerazione della cartilagine articolare mediante tecniche mininvasive” for financial support. Fulvio Ferrante and Alessia Provenzano are greatly acknowledged for their technical help.

References

Almdal, K., Dyre, J., Hvidt, S., & Kramer, O. (1993). Towards a phenomenological definition of the term gel. *Polymer Gels & Networks*, *1*, 5–18.
Baek, M. H., Yoo, B., & Lim, S.-T. (2004). Effects of sugars and sugar alcohols on thermal transition and cold stability of corn starch gel. *Food Hydrocolloids*, *18*, 133–142.
Birch, N. P., & Schiffman, J. D. (2014). Characterization of self-assembled polyelectrolyte complex nanoparticles formed from chitosan and pectin. *Langmuir*, *2014*, 3441–3447.
Bulone, D., Giacomazza, D., Manno, M., Martorana, V., & San Biagio, P. L. (2010). Sucrose pectin interaction from solution to gels. In C. S. Hollingworth (Ed.), *Food hydrocolloids. Characteristics, properties and structures* (pp. 225–241). New York: Nova Science Publisher (Chapter 8).
Chajra, H., Rousseau, C. F., Cortial, D., Ronziere, M. C., Herbage, D., & Mallein-Gerin, F. (2008). Collagen-based biomaterials and cartilage engineering. Application to osteochondral defects. *Bio-medical Materials and Engineering*, *18*, 33–45.
Chen, Y., & Zhang, Y. (2011). Fluorescent quantification of amino-groups on silica nanoparticle surfaces. *Analytical and Bioanalytical Chemistry*, *399*, 2505–2509.
Coimbra, M. A., Barros, A., Barros, M., Rutledge, D. N., & Delgadillo, I. (1998). Multivariate analysis of uronic acid and neutral sugars in whole pectic samples by FT-IR spectroscopy. *Carbohydrate Polymers*, *37*(3), 241–248.
Collins, M. N., & Birkinshaw, C. (2013). Hyaluronic acid based scaffolds for tissue engineering—A review. *Carbohydrate Polymers*, *92*, 1262–1279.
Croisier, F., & Jerome, C. (2013). Chitosan-based biomaterials for tissue engineering. *European Polymer Journal*, *49*, 780–792.
Dispenza, C., Battaglia, G., Giammona, G., Licciardi, M., & Spadaro, G. (2005). *Colloid and Polymer Science*, *284*, 151–159.
Dispenza, C., Alessi, S., & Spadaro, G. (2009). Carbon fiber composites cured by γ-radiation-induced polymerization of an epoxy resin matrix. *Advances in Polymer Technology*, *27*, 163–171.
Dispenza, C., Ricca, M., Lo Presti, C., Battaglia, G., La Valle, M., Giacomazza, D., & Bulone, D. (2010). E-beam irradiation and UV photocrosslinking of microemulsion-laden poly(*N*-vinyl-2-pyrrolidone) hydrogels for in situ encapsulation of volatile hydrophobic compounds. *Polymer Chemistry*, *2*, 192–202.
Dispenza, C., Grimaldi, N., Sabatino, M.-A., Todaro, S., Bulone, D., Giacomazza, D., Przybytniak, G., Alessi, S., & Spadaro, G. (2012). Studies of network organization and dynamics of e-beam crosslinked PVPs: From macro to nano. *Radiation Physics and Chemistry*, *81*, 1349–1353.
Glowacki, J., & Mizuno, S. (2008). Collagen scaffold for tissue engineering. *Biopolymers*, *89*, 338–344.
Grant, G. T., Morris, E. R., Rees, D. A., Smith, P. J. C., & Thom, D. (1973). Biological interactions between polysaccharides and divalent cations: The egg box model. *FEBS Letters*, *32*, 195–198.
Grillet, A. M., Wyatt, N. B., & Gloe, L. M. (2012). Polymer gel rheology and adhesion. In Juan De Vicente (Ed.), *Rheology* (pp. 59–80). Rijeka, Croatia: InTech. Available from: http://www.intechopen.com/books/rheology.
Holme, K., & Hall, L. (1992). Preparation and characterization of *N*-[2-(glycosyloxy)-ethyl]chitosan derivatives. *Carbohydrate Research*, *225*, 291–306.
Hori, Y., Winans, A. M., & Irvine, D. J. (2009). Modular injectable matrices based on alginate solution/microsphere mixtures that gel in situ and co-deliver immunomodulatory factors. *Acta Biomaterialia*, *5*, 969–982.
Karp, J. M., & Langer, R. (2007). Development and therapeutic applications of advanced biomaterials. *Current Opinion in Biotechnology*, *18*, 454–459.

Kavanagh, G. M., & Ross-Murphy, S. B. (1998). Rheological characterization of polymer gels. *Progress in Polymer Science*, *23*, 533–562.
Kurita, K., Akao, H., Kobayash, M., Mori, T., & Nishiyama, Y. (1997). Regioselective introduction of b-galactoside branches into chitosan and chitin. *Polymer Bulletin*, *39*, 543–549.
Kurita, K., Akao, H., Yang, J., & Shimojoh, M. (2003). Nonnatural branched polysaccharides: Synthesis and properties of chitin and chitosan having disaccharide maltose branches. *Biomacromolecules*, *4*, 1264–1268.
Lanza, R. P., Langer, R., & Vacanti, J. (2000). *Principles of tissue engineering*. San Diego, CA: Academic Press.
Leach, J., Bivens, K., Patrick, C. W., & Schmidt, J. C. (2003). Photocrosslinked hyaluronic acid hydrogels: Natural, biodegradable tissue engineering scaffolds. *Biotechnology and Bioengineering*, *82*, 578–589.
Lee, Y., Chung, H. J., Yeo, S., Ahn, C.-H., Lee, H., Messersmith, P. B., & Park, T. G. (2010). Thermo-sensitive, injectable, and tissue adhesive sol–gel transition hyaluronic acid/pluronic composite hydrogels prepared from bio-inspired catechol–thiol reaction. *Soft Matter*, *6*, 977–983.
Lefebvre, J., & Doublier, J. L. (2005). Rheological behavior of polysaccharides aqueous systems. In S. Dumitriu (Ed.), *Polysaccharides: Structural diversity and functional versatility* (2nd ed., pp. 357–381). New York, NY: Marcel Dekker.
Lei, Y., Rahim, M., Ng, Q., & Segura, T. (2011). Hyaluronic acid and fibrin hydrogels with concentrated DNA/PEI polyplexes for local gene delivery. *Journal of Controlled Release*, *153*, 255–261.
Mishra, R. K., Banthia, A. K., & Majeed, A. B. A. (2012). Pectin based formulations for biomedical applications: A review. *Asian Journal of Pharmaceutical and Clinical Research*, 2012, 1-7).
Morris, G. A., Foster, T. J., & Harding, S. E. (2000). The effect of the degree of esterification on the hydrodynamic properties of citrus pectin. *Food Hydrocolloids*, *14*, 227–325.
Munarin, F., Guerreiro, S. G., Grellier, M. A., Tanzi, M. C., Barbosa, M. A., Petrini, P., & Granja, P. L. (2011). Pectin-based injectable biomaterials for bone tissue engineering. *Biomacromolecules*, *12*, 568–577.
Muzzarelli, R. A. A. (1977). *Chitin*. Oxford: Pergamon.
Muzzarelli, R. A. A., & Muzzarelli, C. (2009). Chitin and chitosan hydrogels. In G. O. Phillips, & P. A. Williams (Eds.), *Handbook of hydrocolloids* (pp. 849–888). Boca Raton, FL: CRC Press.
Muzzarelli, R. A. A. (2012). Nanochitins and nanochitosans, paving the way to eco-friendly and energy-saving exploitation of marine resources. *Polymer Science*, *10*, 153–164 (A Comprehensive Reference).
Muzzarelli, R. A. A., Boudrant, J., Meyer, D., Manno, N., De Marchis, M., & Paoletti, M. G. (2012). Current views on fungal chitin/chitosan, human chitinases, food preservation, glucans, pectins and inulin: A tribute to Henri Braconnot, precursor of the carbohydrate polymers science, on the chitin bicentennial. *Carbohydrate Polymers*, *87*, 995–1012.
Oakenful, D. G. (1991). The chemistry of high methoxyl pectins. In R. H. Walters (Ed.), *The chemistry and technology of pectins*. New York, NY: Academic Press.
Pitarresi, G., Giacomazza, D., Triolo, D., Giammona, G., & San Biagio, P. L. (2012). Rheological characterization and release properties of inulin-based hydrogels. *Carbohydrate Polymers*, *88*, 1033–1040.
Ravi Kumar, M. N. V., Muzzarelli, R. A. A., Muzzarelli, C., Sashiwa, H., & Domb, A. J. (2004). Chitosan chemistry and pharmaceutical perspectives. *Chemical Reviews*, *104*, 6017–6084.
Rinaudo, M. (2006). Chitin and chitosan: Properties and applications. *Progress in Polymer Science*, *31*, 603–632.
Ross-Murphy, S. B. (1995). Rheological characterisation of gels. *Journal of Texture Studies*, *26*, 391–400.
Sabatino, M.-A., Bulone, D., Veres, M., Spinella, A., Spadaro, G., & Dispenza, C. (2013). Structure of e-beam sculptured poly(*N*-vinylpyrrolidone) networks across different length-scales, from macro to nano. *Polymer*, *54*, 54–64.
Seidlits, S. K., Drinnan, C. T., Petersen, R. R., Shear, J. B., Suggs, L. J., & Schmidt, C. E. (2011). Fibronectin–hyaluronic acid composite hydrogels for threedimensional endothelial cell culture. *Acta Biomaterialia*, *7*, 2401–2409.
Sokolsky-Papkov, M., Agashi, K., Olaye, A., Shakeshef, K., & Domb, A. J. (2007). Polymer carriers for drug delivery in issue engineering. *Advanced Drug Delivery Reviews*, *30*, 187–206.
Toome, V., & Manhart, K. (1975). A simple simultaneous colorimetric determination of primary and secondary amines with fluorescamine. *Analytical Letters*, *8*, 441–448.
Wang, Z. Y., Zhang, Q.-Z., Konno, M., & Saito, S. (2004). Sol–gel transition of alginate solution by the addition of various divalent cations: ^{13}C NMR spectroscopic study. *Biopolymers*, *33*, 703–711.
Wang, C. C., Yang, K. C., Lin, K. H., Liu, H. C., & Lin, F. H. (2011). A highly organized three-dimensional alginate scaffold for cartilage tissue engineering prepared by microfluidic technology. *Biomaterials*, *32*, 7118–7126.
Yalpani, M., & Hall, L. D. (1984). Some chemical and analytical aspects of polysaccharide modifications. 3. Formation of branched-chain, soluble chitosan derivatives. *Macromolecules*, *17*, 272–281.
Yamada, H. (1996). Contribution of pectins on health care. In J. Visser, & A. G. J. Voragen (Eds.), *Pectins and pectinases* (pp. 173–190). Amsterdam: Elsevier.